

# Patterned interrogation scheme for compressed sensing photoacoustic imaging using a Fabry Perot planar sensor

Nam Huynh<sup>1</sup>, Edward Zhang<sup>1</sup>, Marta Betcke<sup>2</sup>, Simon Arridge<sup>2</sup>, Paul Beard<sup>1</sup> and Ben Cox<sup>1</sup>

<sup>1</sup>Department of Medical Physics and Bioengineering, University College London, WC1E 6BT. UK

<sup>2</sup>Department of Computer Science, University College London, WC1E 6BT. UK

## ABSTRACT

Photoacoustic tomography (PAT) has become a powerful tool for biomedical imaging, particularly pre-clinical small animal imaging. Several different measurement systems have been demonstrated, in particular, optically addressed Fabry-Perot interferometer (FPI) sensors have been shown to provide exquisite images when a planar geometry is suitable. However, in its current incarnation the measurements must be made at each point sequentially, so these devices therefore suffer from slow data acquisition time. An alternative to this point-by-point interrogation scheme, is to interrogate the whole sensor with a series of independent patterns, so each measurement is the spatial integral of the product of the pattern and the acoustic field (as in the single-pixel Rice camera). Such an interrogation scheme allows compressed sensing to be used. This enables the number of measurements to be reduced significantly, leading to much faster data acquisition. An experimental implementation will be described, which employs a wide NIR tunable laser beam to interrogate the FPI sensor. The reflected beam is patterned by a digital micro-mirror device, and then focused to a single photodiode. To demonstrate the idea of patterned and compressed sensing for ultrasound detection, a scrambled Hadamard operator is used in the experiments. Photoacoustic imaging experiments of phantoms shows good reconstructed results with 20% compression.

Keywords: Photoacoustic imaging, Fabry-Perot interferometer, digital micromirror device, compressed sensing

## 1. INTRODUCTION

Fabry-Perot (FP) polymer film ultrasound sensors can detect acoustic waves over a bandwidth of many tens of MHz [1]. By interrogating the sensors with a focussed beam, and scanning point-to-point, it is possible to synthesise arrays of many tens of thousands of points with small element sizes with sensitivities of a few hundred Pa. For these reasons, it has proved ideal for preclinical small animal photoacoustic imaging. However, the scanning of the beam is time-consuming, and images can take several minutes to acquire. For capturing dynamic changes, and for avoiding movement artifacts, it is necessary to be able to acquire the data more quickly. One possibility might be to use a multi-element detector array, such as a CCD camera, to interrogate the FP sensor, but no cameras exist that can sample at the tens of MHz required for the bandwidths of photoacoustic signals. This paper explores the possibility of using compressed sensing to speed up the measurement of the data.

## 2. COMPRESSED SENSING

Image compression, ubiquitous in today's world, is based on the idea that it is possible to find a basis in which the image can be represented much more sparsely than in the pixel basis. In other words, the image can be represented with many fewer coefficients than pixels. The widespread use of the JPEG-2000 format, which stores images sparsely in a wavelet basis, is perhaps the best known example. Once an image has been compressed it takes up less memory than the original image. However, in this example it is necessary to store the whole uncompressed image before compressing it. Compressed sensing, or compressive sampling, tries to avoid this, by measuring the coefficients in the sparse basis directly [2]. This has two significant advantages: as well as not having to store all the uncompressed data, it is also not necessary to measure it, so fewer measurements are needed to obtain all the information in the data. It is the latter advantage, and the accompanying speed-up, that is of principal interest here.

## 2.1 Compressed Measurements

The acoustic field at the FP sensor at time  $t$  will be denoted by  $p(x, y, t)$ . A point-by-point scanner scans  $N$  points on the FP sensor, and measures an acoustic pressure time series of  $T$  samples at each, resulting in the data set  $P \in \mathbb{R}^N \times \mathbb{R}^T$ , which it will be useful to write as a collection of measurements  $P = \{p_t, t = 0, \dots, T - 1\}$  where  $p_t = \{p_t^n, n = 1, \dots, N\} \in \mathbb{R}^N$  represents the measurements at the  $N$  pixels at a single time  $t$ , and  $p_t^n = p(x_n, y_n, t)$  the scalar measurement amplitude at a single point on the sensor with coordinates  $(x_n, y_n)$  at time  $t$ . If, for a single time  $t$ , the pressure field  $p_t$  can be represented sparsely in a basis,  $\Psi$ , then we can write

$$\begin{bmatrix} p_t^1 \\ \vdots \\ p_t^N \end{bmatrix} = \begin{bmatrix} \psi_1^1 & \cdots & \psi_M^1 \\ \psi_1^2 & \cdots & \psi_M^2 \\ \vdots & \vdots & \vdots \\ \psi_1^N & \cdots & \psi_M^N \end{bmatrix} \begin{bmatrix} a_t^1 \\ \vdots \\ a_t^M \end{bmatrix}, \quad p_t = \Psi a_t \quad (1)$$

where the columns  $\psi_m$  are the basis functions of the sparse basis  $\Psi$ , and  $a_t = \{a_t^m, m = 1, \dots, M < N\}$  are the corresponding coefficients. If the full measurements  $p_t$  were known then it would be possible to calculate the sparse coefficients using an inner product  $a_t^m = \langle \psi_m, p_t \rangle$ . However, the aim of compressed sensing is to obtain the coefficients  $a_t$  *directly from  $M$  measurements*, thereby eliminating the intermediate storage requirements, and – more importantly here – reducing the data acquisition time significantly.

In compressed sensing, rather than measuring at single points (point-by-point scanning), we measure integrals over patterns, or collections of points. In other words we measure the set of amplitudes  $w_t = \{w_t^m, m = 1, \dots, M\}$  given by

$$w_t^m = \langle \phi_m, p_t \rangle, \quad m = 1, \dots, M \quad (2)$$

where the  $\phi_m$  are measurement patterns. The idea behind compressed sensing is to assume that  $p_t$  is *sparsely* represented in a basis  $\Psi$  and use measurement patterns  $\phi_m$  which are *incoherent* to the basis vectors  $\psi_m$ . The incoherence of the basis  $\Psi$  and the patterns  $\Phi$  is crucial. If one knew, ahead of time, which sparse coefficients represented the solution, we could coherently measure the relevant  $\psi_m$  by using them as the measurement patterns,  $\phi_m = \psi_m$ . This is, however, never the case in practice, therefore we use patterns which through their incoherence ‘equally’ sense all the basis vectors  $\psi_m$ , and afterwards use sparse recovery to extract the sparse coefficients from these measurements.

For the proof-of-principle results reported here, the measurement matrix (the rows of which are the measurement patterns  $\phi_m$ ) was chosen as a scrambled Hadamard matrix which is known to behave similarly to a random Bernoulli matrix and, in contrast to the latter, can also be applied efficiently. The sparsity basis was chosen to be the Hadamard basis. Experimentally it was not possible to implement  $(-1,1)$  Hadamard patterns, so  $(0,1)$  patterns were used, and the mean value of all the time series was subtracted from the set. In this way, the amplitudes,  $w_t^m$ , were measured for a subset of scrambled Hadamard patterns. This choice was not made because we believe the data  $p_t$  to be especially sparse in the Hadamard basis, but for practical reasons: the binary square patterns are easy to implement experimentally, and a Fast Hadamard Transform exists, which is advantageous both in terms of memory and reconstruction speed. Future work will explore alternative bases in which the field may be expected to be particularly sparse, and alternative measurement patterns, notably localised and sparse patterns.

## 2.2 Reconstruction

There are two stages to the image reconstruction. First, the data at each time step,  $p_t$ , must be estimated from the measured amplitudes,  $w_t$ , and then the photoacoustic image must be reconstructed. The first part was solved here, non-optimally but efficiently, by using the Fast Hadamard Transform with the missing data set to zero. While this is not ‘sparse recovery’, it demonstrates that the sparse recovery will work. It shows that using random subsampling causes the aliasing artefacts to appear scrambled, noise-like, and therefore subsequent denoising can be efficiently accomplished using sparse recovery algorithms, which will be considered in future work. The image reconstruction was then implemented using time reversal [3].

### 3. PHOTOACOUSTIC IMAGING

The experimental setup is illustrated in Fig 1(a). The FPI sensor (aluminium coatings, parylene spacer, 50 $\mu$ m thickness) was illuminated by a 20mm diameter expanded interrogation beam (Santec TSL-510 tunable laser source connected to a IPG Laser GmbH Erbium Fiber Amplifier EAD-4-L). The reflected beam from the sensor was then redirected to the digital micromirror device, or DMD, (ViaLUX V-7000 DLP 0.7" XGA 1024x768 array, 13.68 $\mu$ m pitch size) by the polarised beam splitter (Thorlabs CM1-PBS254). To the coherent incident light, the DMD acts like a two-dimensional diffraction grating and the reflected light is shared among many orders [4]. The DMD was placed so that the angles of incident light and the strongest diffraction order ( $\sim$ 70% power) are 24 $^\circ$  and  $\sim$ 47 $^\circ$ . The output diffracted beam was collected by a lens (focal length 25.4mm) and focused into a customised InGaAs photodiode (G8376-03). The photodiode output was connected to an oscilloscope (NI PCI-5114 digitiser, sampling rate 50MHz) for data acquisition. A LABVIEW program was written to control the whole system. In this experimental arrangement, the DMD patterned the beam reflected from the sensor, and directed it to the photodiode. The patterns were sequentially displayed on the DMD, and for each pattern a time series was recorded. The active area on the DMD was chosen to be 640x640 pixels ( $\sim$ 8.7x8.7 mm $^2$ ) and positioned to match the most uniformly sensitive region on the FP sensor. The arrangement for the photoacoustic experiments is shown in Fig. 1 (b).

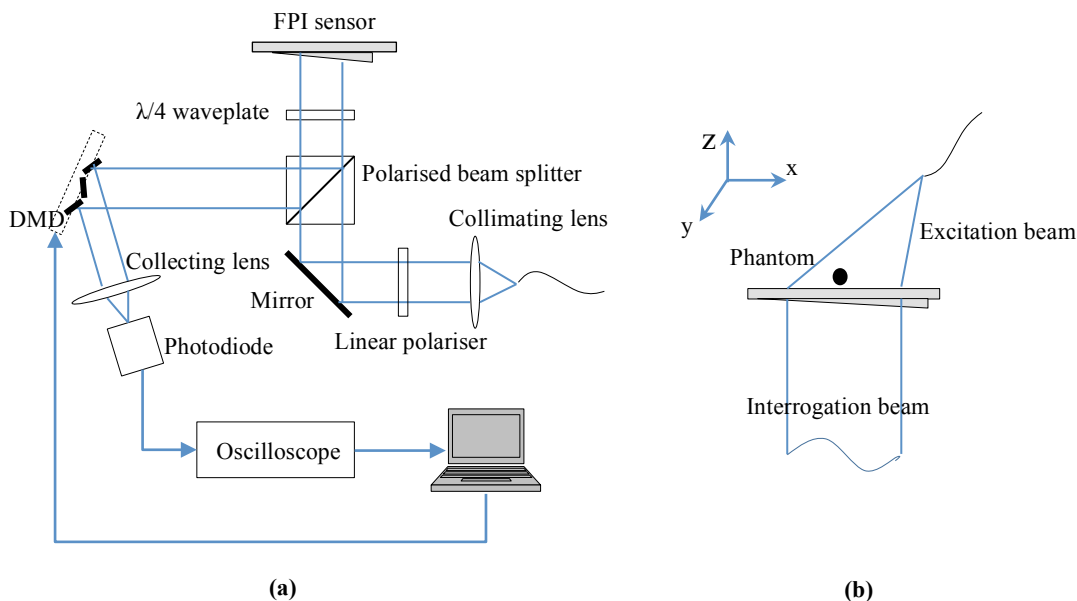


Figure 1. (a) Experimental setup, (b) Photoacoustic imaging arrangement.

The DMD-interrogated sensor was used to obtain photoacoustic images of phantom absorbers. Q-switched 10ns pulses from a fiber-coupled Nd:YAG laser (Continuum Minilite-20, 20Hz repetition rate) was used for the photoacoustic excitation. The measured power at the fiber output was 17.2mJ. As the aluminium FP sensor is not transparent to the 1064nm wavelength, the excitation light was delivered from above the phantom, as indicated in Fig. 1(b). Scrambled Hadamard patterns with 128x128 pixels were used for these experiments, so each image pixel corresponded to a group of 5x5 micromirrors on the DMD. The two phantoms are shown in Fig 2(a) and 2(b). A knotted artificial hair, 2(a), and a twisted polymer ribbon, 2(b), were immersed in 1% Intralipid and positioned approximately 2 mm above the detection plane and 3mm under the Intralipid surface. The diameter of the hair was  $\sim$ 150  $\mu$ m and the ribbon width was  $\sim$ 350  $\mu$ m.

Figure 3 shows maximum intensity projections of the photoacoustic images of the phantoms shown in Fig. 2. The images (from left to right both rows) were obtained using 100%, 50% and 20% of the scrambled Hadamard patterns, demonstrating good image quality with a significant level of compression. The main features of the targets are recovered successfully even with 20% compression. Planar reconstructions in general suffer from limited view artifacts, which here take the form of blurring the sides of the targets making them appear slightly larger than their true size, and the lack of visibility (due to parts of the acoustic wave propagating parallel or close to parallel to the sensor surface) causes the vertical regions of the phantoms to be poorly reconstructed.

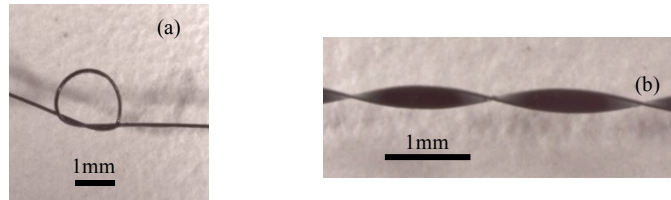


Figure 2. Phantoms for photoacoustic imaging experiments: (a) artificial hair (~150  $\mu\text{m}$  in diameter); (b) twisted black polymer ribbon (~350  $\mu\text{m}$ )

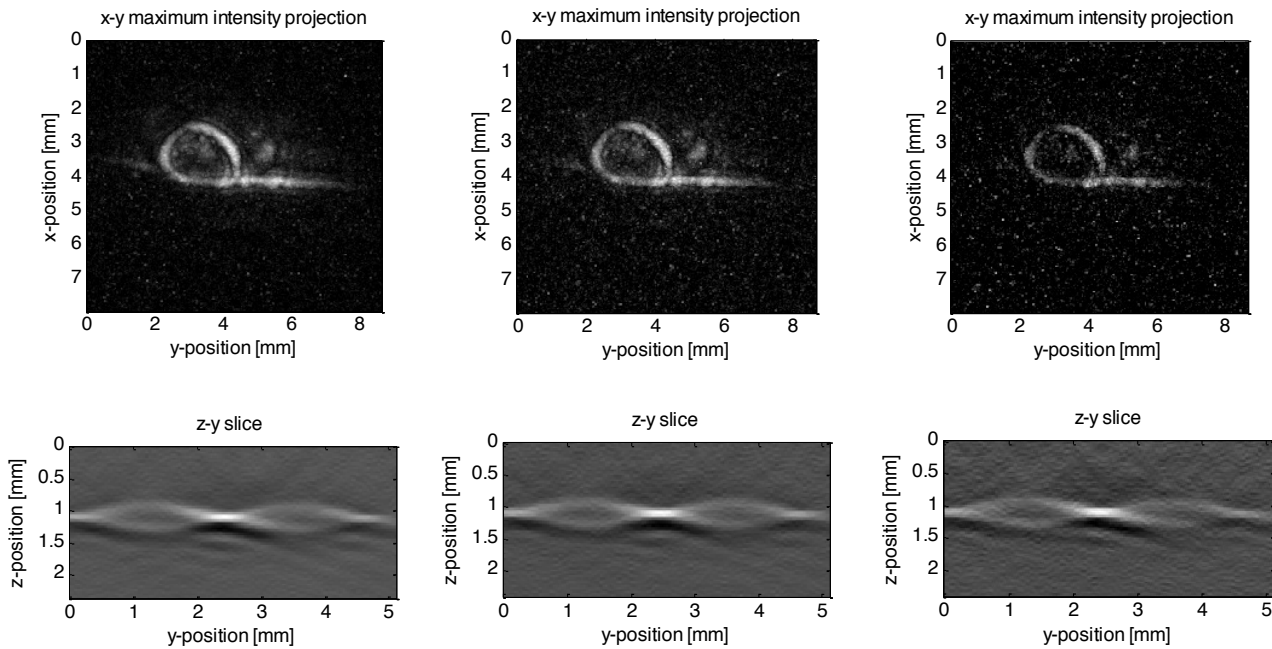


Figure 3. Compressed sensing photoacoustic images. First row, left to right: image of knotted hair without compression – with 50% compression – with 20% compression. Second row, left to right: image of the twisted polymer ribbon without compression – with 50% compression – with 20% compression.

## 4. DISCUSSION

The term ‘compressed sensing’ has been used previously in photoacoustic imaging in two senses. In the first, it refers to two-dimensional photoacoustic imaging using patterned *excitation* light, an idea which will not extend to 3D PAT [5-7], and which is quite different from the patterned compressed sensing described here. In the second, the notion that PAT images can be represented sparsely in some basis has been used to regularise image reconstructions from spatially undersampled data [8-12]. However, the sensors used in these studies are restricted to point sampling, and cannot optimise the compression by exploiting different – eg. random – measurement patterns, as can be done with our experimental set-up. Our study shows the possibility of improving acquisition speed in photoacoustic imaging with a planar array, by exploiting ideas from compressed sensing. These preliminary results show that, even just using scrambled Hadamard patterns, a little as 20% of the data is sufficient to generate an image. The design of the system is such that it is capable of employing almost any measurement patterns, and further optimisation is therefore possible.

## 5. CONCLUSION

Compressed sensing photoacoustic imaging has been demonstrated with patterned ultrasonic detection, by using a DMD to interrogate a planar Fabry Perot ultrasound sensor. As a first demonstration, scrambled Hadamard patterns were used to sample the pressure field on the sensor. Images were obtained, without significant loss of quality, to a compression of 20% (ie. data equivalent to 20% of the full data was used in the reconstruction).

## REFERENCES

- [1] E. Zhang, J. Laufer, & P. Beard, "Backward-mode multiwavelength photoacoustic scanner using a planar Fabry-Perot polymer film ultrasound sensor for high-resolution three-dimensional imaging of biological tissues," *Appl. Opt.* 47, 561-577 (2008)
- [2] E. Candès & M. Wakin, "An introduction to compressive sampling", *IEEE Signal Processing Magazine*, 25(2), 21 - 30 (2008)
- [3] B.E. Treeby & B.T. Cox, "*k*-Wave: MATLAB toolbox for the simulation and reconstruction of photoacoustic wave fields", *J. Biomed. Opt.*, 15(2), 021314 (2010)
- [4] Texas Instruments, *Using Lasers with DLP DMD Technology*, (2008)
- [5] D. Liang, H.F. Zhang & L. Ying, "Compressed-sensing Photoacoustic Imaging based on random optical illumination." *Int. J. Func. Inform. Person. Med.*, 2(4), 394–406 (2009)
- [6] M. Sun, N. Feng, Y. Shen et al., "Photoacoustic imaging method based on arc-direction compressed sensing and multi-angle observation", *Opt. Express*, 19(16), 14801–14806 (2011)
- [7] M. Sun, N. Feng, Y. Shen et al., "Photoacoustic image reconstruction based on Bayesian compressive sensing algorithm", *Chinese Optics Letters*, 9(6), 061002 (2011)
- [8] J. Provost & F. Lesage, "The Application of Compressed Sensing for Photo-Acoustic Tomography", *IEEE Trans. Med. Imag.*, 28(4), 585-594 (2009)
- [9] Z. Guo, C. Li, L. Song & L.V. Wang, "Compressed sensing in photoacoustic tomography in vivo", *J. Biomed. Opt.* 15(2), 021311 (2010)
- [10] J. Meng, L. Wang, L. Ying, D. Liang & L. Song, "Compressed-sensing photoacoustic computed tomography in vivo with partially known support," *Opt. Express*, 20, 16510-16523 (2012).
- [11] J.G. Wang et al., "Compressed sensing in microwave induced thermo-acoustic tomography", 2012 Int. Conf. Comp. Problem-Solving (ICCP), 310–314 (2012)
- [12] Y. Zhang, Y. Wang & C. Zhang, "Total variation based gradient descent algorithm for sparse-view photoacoustic image reconstruction". *Ultrasonics*, 52(8), 1046–55 (2012)